J Neurophysiol 91: 301–313, 2004.
First published October 1, 2003; 10.1152/jn.00022.2003.

Information Content of Auditory Cortical Responses to Time-Varying Acoustic Stimuli

Thomas Lu and Xiaoqin Wang
Laboratory of Auditory Neurophysiology, Department of Biomedical Engineering, Johns Hopkins University School of Medicine, Baltimore, Maryland 21205

Submitted 10 January 2003; accepted in final form 26 September 2003

Lu, Thomas and Xiaoqin Wang. Information content of auditory cortical responses to time-varying acoustic stimuli. *J Neurophysiol* 91: 301–313, 2004. First published October 1, 2003; 10.1152/jn.00022.2003. The present study explores the issue of cortical coding by spike count and timing using statistical and information theoretic methods. We have shown in previous studies that neurons in the auditory cortex of awake primates have an abundance of sustained discharges that could represent time-varying signals by temporal discharge patterns or mean firing rates. In particular, we found that a subpopulation of neurons can encode rapidly occurring sounds, such as a click train, with discharges that are not synchronized to individual stimulus events, suggesting a temporal-to-rate transformation. We investigated whether there were stimulus-specific temporal patterns embedded in these seemingly random spike times. Furthermore, we quantitatively analyzed the precision of spike timing at stimulus onset and during ongoing acoustic stimulation. The main findings are the following. *1*) Temporal and rate codes may operate at separate stimulus domains or encode the same stimulus domain in parallel via different neuronal populations. *2*) Spike timing was crucial to encode stimulus periodicity in "synchronized" neurons. *3*) "Nonsynchronized" neurons showed little stimulus-specific spike timing information in their responses to time-varying signals. Such responses therefore represent processed (instead of preserved) information in the auditory cortex. And *4*) spike timing on the occurrence of acoustic events was more precise at the first event than at successive ones and more precise with sparsely distributed events (longer time intervals between events) than with densely packed events. These results indicate that auditory cortical neurons mark sparse acoustic events (or onsets) with precise spike timing and transform rapidly occurring acoustic events into firing rate-based representations.

INTRODUCTION

The auditory system can process acoustic stimuli that vary on a rapid time scale. How these rapid acoustic transients are represented by neural discharges in the auditory pathway remains a challenging question. Neurons that fire action potentials in response to particular events in a time-varying sound exhibit what can be called stimulus-synchronization, but this activity is generally limited, if not absent, in response to a rapid sequence of acoustic transients. This has been well documented in the literature for both peripheral and central auditory pathways (Creutzfeldt et al. 1980; de Ribaupierre et al. 1972; Eggermont 1991; Goldstein et al. 1959; Johnson 1980; Joris and Yin 1992; Langner 1992; Lu et al. 2001b; Phillips et al. 1989). Although rate coding is not a new hypothesis (e.g., Adrian and Zotterman 1926), the question of its usefulness in the auditory cortex may be due, in part, to the lack of sustained discharges in the auditory cortex under commonly used anesthetic conditions. Representations of time-varying stimuli by average discharge rates in the auditory system are being revisited as a viable method of cortical encoding (Bieser and Müller-Preuss 1996; Liang et al. 2002; Lu et al. 2001a,b; Wang et al. 2003). Studies on the auditory cortex of awake animals demonstrate that neurons can and do show sustained and vigorous responses to a wide variety of acoustic stimuli (Barbour and Wang 2002; Bieser and Müller-Preuss 1996; de Charms et al. 1998; Liang et al. 2002; Lu et al. 2001a,b; Malone et al. 2002; Recanzone 2000; Wang et al. 2003; Whitfield and Evans 1965).

How much cortical representation of stimuli is based on spike count and how much on spike timing is an ongoing debate in the literature. Temporal codes can range from the timing of individual spikes such as first spike latency (e.g., Heil 1997a; Phillips and Hall 1990) to patterns of neural activity, such as stimulus-synchronized discharges (de Ribaupierre et al. 1972; Goldstein et al. 1959), and to even more complex temporal patterns. It is important to distinguish between temporal coding of "when" and "what" events occurred (Borst and Theunissen 1999). The former, such as stimulus-synchronized discharges, provides information that directly correlates to the time a stimulus feature occurred. The latter cortical representation maps a specific stimulus feature to a temporal discharge pattern, such as odors in the olfactory system (Laurent et al. 1996) or two-dimensional visual patterns in primate inferior temporal cortex (Optican and Richmond 1987).

Traditionally, temporal discharge patterns have been analyzed using methods such as autocorrelation or synchronization index (based on vector strength). More recently, information theory has been applied to address the issue of rate codes versus temporal codes. In auditory cortex of cat, Furukawa and Middlebrooks (2002) showed that full-spike patterns contained more information on stimulus locations than did spike counts and that transmitted information was sensitive to disruption of spike timing on a scale of more than ~4 ms. In the rat somatosensory cortex, it was shown that spike timing could increase the information content by 44% compared with spike count alone (Panzeri et al. 2001). The timing of the first spike was the largest contributor to the information content based on spike timing. In the LGN of the visual pathway, it was demonstrated that temporal patterns can contain redundant information, but more often they coded additional visual informa-

Address for reprint requests and other correspondence: X. Wang, Dept. of Biomedical Engineering, Johns Hopkins University School of Medicine, 720 Rutland Ave., Ross 424, Baltimore, MD 21205 (E-mail: xwang@bme.jhu.edu).

The costs of publication of this article were defrayed in part by the payment of page charges. The article must therefore be hereby marked "*advertisement*" in accordance with 18 U.S.C. Section 1734 solely to indicate this fact.

tion (up to 24.9% more of the total information content) (Reinagel and Reid 2000). Buracas et al. (1998) showed that high temporal precision rather than low spike count variability accounted for high information rates.

In our recent studies in awake marmosets, we have shown that a population of auditory cortical neurons could code rapid temporal modulations of sounds by the magnitude of their average discharge rates and that slow modulations of sounds were reflected in another population by their stimulus-synchronized temporal discharge patterns (Liang et al. 2002; Lu et al. 2001a,b; Wang et al. 2003). These auditory cortical responses to time-varying sounds demonstrated the capacity of cortical coding based on average discharge rates. Although there was little evidence of stimulus-synchronized activity in the responses to the rapid temporal modulations in many cortical neurons, the question of whether such neurons had additional information in their non-stimulus-synchronized discharge patterns was not addressed. Vector strength measures used in our previous studies were unable to reveal intrinsic temporal patterns that were not synchronized to the stimulus waveform. Thus it remained unclear if cortical neurons lacking stimulus-synchronized discharges were temporally encoding the stimuli in other ways. In this report, we use statistical and information-theoretic methods (Shannon 1948) to quantify the responses of auditory cortical neurons to time-varying stimuli. The present study demonstrates that, regarding how auditory cortical neurons encode time-varying signals, it is not simply an issue of whether spike timing is important, but *when* it is important (i.e., under what stimulus conditions and in which population of cortical neurons).

METHODS

Animal preparation and recording procedures

Animal preparation and recording procedures were detailed in a previous report (Lu et al. 2001a) and are only briefly described here. Marmoset monkeys (*Callithrix jacchus*), a highly vocal New World primate (Wang 2000), were adapted to sit quietly in a semi-restraint device through an acclimation period of several weeks. The primary auditory cortex (A1) of the marmoset lies largely on the surface of the superior temporal gyrus (Aitkin et al. 1986), and our procedure approaches A1 laterally through small holes (~1.0 mm) (Lu et al. 2001a). All necessary precautions and steps were taken to ensure both animal comfort and sterility during all procedures. All experimental procedures were approved by the Institutional Animal Care and Use Committee of the Johns Hopkins University following NIH guidelines.

Single-unit activity was recorded using tungsten microelectrodes of impedance ranging from 2 to 5 MΩ (A-M Systems). For each cortical site, the electrode was inserted nearly perpendicular, under visual guidance with an operating microscope, to the cortical surface by a micromanipulator (Narishige) and advanced by a hydraulic microdrive (David Kopf Instruments). Action potentials were detected by a template-based spike sorter (MSD, Alpha Omega Engineering) and continuously monitored by the experimenter while data recordings progressed. Typically, one to three well-isolated single neurons were studied in each session. The data presented were mainly obtained from A1 and may include a small number of neurons from immediately adjacent areas. Single neurons were encountered at all cortical layers, but the majority of the recorded data were from upper layers, and to a lesser extent, from middle layers, judging by the depth of recording and response characteristics. The location of A1 was determined by its tonotopic organization, its relationship to the lateral belt area (which was more responsive to noises than tones), and by its response properties (short latencies, and highly responsive to tones).

Acoustic stimuli

All recording sessions were conducted within a double-walled, sound-proof chamber (Industrial Acoustics). Acoustic signals were generated digitally and delivered in free-field through a speaker located ~1 m in front of the animal. The characteristic frequencies (CFs) and thresholds were precisely determined by a computer-controlled stimulus protocol. Once a neuron was isolated and its basic response properties determined (e.g., CF, latency and rate-level characteristics), other stimulus protocols were executed in randomized blocks for 5 or 10 repetitions. Spontaneous activity was recorded for 500 ms before and after each trial. Intertrial intervals were ≥1.5 s long. For all stimuli, sound intensity was typically set at the peak in the neuron's rate-level function if it was nonmonotonic or 10–30 dB above threshold if it was monotonic.

Acoustic stimuli used were click-trains with regular or irregular (Poisson-distributed) interclick intervals (ICIs) (Lu and Wang 2000; Lu et al. 2001b), ramped and damped sinusoids (Lu et al. 2001a; Patterson 1994), and sinusoidal amplitude-modulated (sAM) tones (Liang et al. 2002). The click trains with regular ICIs (*regular click trains*) had fixed intervals ranging from 3 to 100 ms and consisted of either broad-band (*rectangular*) or narrow-band (*Gaussian*) clicks. The click-trains with irregular ICIs (*irregular click trains*) had random intervals based on a modified Poisson distribution ($\lambda = 70$ ms) with a dead time of 3 ms. Ramped and damped sinusoids were tone carriers that were modulated by an exponentially growing or decaying envelope. The sAM stimuli had modulation frequencies ranging from 2 to 512 Hz. All narrow-band stimuli were centered at the CF of the neuron being studied.

Data analysis

MEAN LATENCY AND COEFFICIENT OF VARIATION. The coefficient of variation, $CV = \sigma/\mu$, of spike time latencies (relative to the click that evoked the response) was used to measure the precision of spike timing. The mean latency, μ, and SD, σ, were calculated from a "postclick" histogram of response. This is similar to the period histogram in that the responses to each click were accumulated into a histogram, but the window-sizes are not necessarily equal to the stimulus period. For synchronized neurons, the window sizes were adjusted manually to include all of the onset response (generally, the 1st cluster of spikes responding to the 1st click) for each neuron. At long ICIs (such as 100 ms), the analysis window was shorter than the ICI. This was done because it provides a possible means to compare the onset response with any potential subsequent responses to the clicks, particularly for responses to the midrange and shorter ICIs. The window size was meant to include the cluster of onset responses and was generally larger than the period at these shorter intervals. The CV of the onset response was calculated from the spikes occurring within the first window (which had been adjusted to include the initial cluster of spikes) and did not include later spike times. Window sizes for nonsynchronized neurons were fixed at 50 ms, as many did not show a clear burst of activity in response to stimulus onset, and there was no obvious selection of a window size. Spike count CV was also analyzed, using the same window sizes as with the spike timing analysis.

INFORMATION MEASURES. We measured the information content of the stimuli based on spike counts, inter-spike intervals (ISI), and period histograms. The entropy of the response is given by the formula

$$H(r) = -\sum_{r} p(r_i) \cdot \log_2 p(r_i)$$

where $p(r_i)$ is the probability of the response r_i occurring in the ith bin of the histogram of the response measure (e.g., ISI or spike count, explained in the following text).

Stimulus-specific mutual information was computed using the following formula

$$I(s, r) = \sum_r p(r_i|s) \cdot \log_2 \frac{p(r_i|s)}{p(r_i)}$$

where r_i is the ith response measure, and s is the stimulus, $p(r_i)$ is the probability of the response r_i occurring, and $p(r_i|s)$ is the conditional probability of r_i occurring given s. $p(r|s)$ is conditioned on the stimulus classified by ranked ICI (i.e., distributions only from 100 ms ICI condition or only from 70 ms ICI condition). When 19 ICI conditions are presented with equal probability, the maximum mutual information is ~4.25 bits.

The response measure for the ISI was based on the time between successive action potentials in a given stimulus presentation trial. The distribution of these ISIs was used as an estimate of their probability of occurrence. Bin widths were 1 ms, and a total of 1,000 bins were used. The total entropy of the response was calculated from the ISI distribution over all stimulus conditions.

Spike count distributions were generated using a sliding window for each trial. The length of the window was chosen to be 100 ms, which was similar to the window size used in another study (Buracas et al. 1998). The distribution of the spike counts, with a bin width of 1 spike and a total of 100 bins, was used in calculating the entropy.

Given the choices of bin widths, the analysis was not sensitive to the total number of bins. Although the maximum theoretical entropy increases with the total number of bins, unoccupied bins add nothing to the entropy calculation (i.e., zero probability of occurrence, and thus no information). For example, two distributions of 100 and 1,000 bins, with 4 occupied bins each (e.g., with 1 count in each bin) and the others empty, will have the same calculated entropy (2 bits).

Because small sample sizes can bias the mutual information (Panzeri and Treves 1996), we implemented a bias correction

$$I_{\text{corrected}} = I_{\text{raw}} - I_{\text{chance}}$$

where I_{raw} is the uncorrected calculated mutual information, and I_{chance} is the mean mutual information that is expected by chance and is bootstrapped by randomly reassigning responses, with replacement, to stimuli over 1,000 iterations. It is then possible to assess the significance of the mutual information based on the bootstrapped distribution. Values of raw mutual information >95% of those in the chance distribution were considered significant.

SPIKE-JITTERING MANIPULATIONS. To measure the amount of temporal information in the responses, we compared the entropy of the response with a temporally modified version of the response. These temporal manipulations were accomplished by two methods. The first was to jitter spike times by adding or subtracting a random amount to or from each time. Spike times across all stimulus conditions were jittered independently according to a uniform distribution with a maximum jitter time of $(\pm 1/2)\Delta t$. The values of Δt were systematically varied from 3 to 100 ms. The entropy calculations in this case were based on period histograms using a bin size of 1 ms.

The second method was to randomize spike times according to a uniform distribution to remove any temporal structure in the response and therefore maximize entropy. Because spike times were randomized rather than added or removed, the discharge rates at the trial-by-trial level were unchanged. The entropy of the ISIs of the control was compared with that of the randomized version. This provided a basis to determine if any difference in the temporal structure of the response was due to the stimuli, and a ratio near 1 indicates that the spike time distribution in the control was as nearly uniform as the randomized version. The ratios of the ISI entropy were averaged over the population for each ICI condition. The temporal structure of the spontaneous activity was analyzed similarly.

RESULTS

Quantitative analyses were based on 86 single units recorded from A1 of four marmosets using regular click trains (Lu et al. 2001b). Of these, 36 responded with stimulus-synchronized discharges (*synchronized* neurons) to click trains, and 50 responded with nonsynchronized discharges (*nonsynchronized* neurons). Cortical responses to time-varying signals with modulations introduced by different means (e.g., regular and irregular click trains, amplitude-modulated tones) (Liang et al. 2002; Lu et al. 2001a,b) were also used in the present study.

Stimulus-synchronized and nonsynchronized temporal discharge patterns of responses to time-varying signals

Figures 1 and 2 illustrate the two types of temporal discharge patterns that we observed in auditory cortex of awake marmosets: stimulus-synchronized and nonsynchronized responses, using a variety of time-varying sounds. For each example, the dot raster (*left*), ISI histogram (*middle*), and conditional ISI plot (*right*) are shown to highlight temporal structures of the recorded spike trains. These examples illustrate several important properties of cortical responses to time-varying signals as analyzed in the following text.

Cortical neurons can operate in different stimulus ranges (i.e., short vs. long ICIs) to represent a stimulus continuum (Fig. 1, *A* vs. *B*). The unit shown in Fig. 1*A* responded to click trains with long ICIs with stimulus-synchronized discharges that are clearly seen as clusters of regularly spaced points. Driven responses at the shorter intervals (<25 ms ICI) were absent in this unit. These units, where the temporal pattern of the click-train stimulus is clearly evident in the response, will be referred to as *synchronized units*. Repeating occurrences of particular ISI values can be revealed by an ISI histogram (Fig. 1*A*, *middle*). For synchronized units, the histogram will have peaks at each ISI value that corresponds to ICIs in a click-train. At 100 ms, there is a clear peak that resulted from the stimulus-synchronized response to the 100-ms ICI click train (Fig. 1*A*, *middle*). The other ICI values (30–75 ms) to which this unit was synchronized have corresponding peaks in the histogram (i.e., the ISI distribution varies with ICI) but appear tightly packed because of the fine spacing between different click-train ICI values tested and some randomness inherent in spike timing precision. The cluster appearing at very short intervals (<5 ms) was a result of bursting.

Because it is possible that the duration of an ISI can be dependent on that of the immediately preceding ISI and thus temporally structuring a unit's discharge pattern, each ISI in the response is plotted against each subsequent ISI (Fig. 1*A*, *right*). The presence of any dependencies in the temporal structure of the response would appear as clusters of data points in the conditional ISI plot as demonstrated by the representative example of a synchronized neuron (Fig. 1*A*, *right*). The regularity of the discharges in response at each click train ICI value resulted in a diagonal band of clusters ranging from 30–100 ms that indicated equal values of preceding and subsequent ISIs. Its range reflects the ICI values to which the unit showed synchronized responses (Fig. 1*A*, *left*). The off diagonal bands result from synchronized responses that skipped a click because they were not 100% entrained, resulting in ISI values that were multiples of the ICI. In addition, there were also a number of clusters in the conditional ISI plot

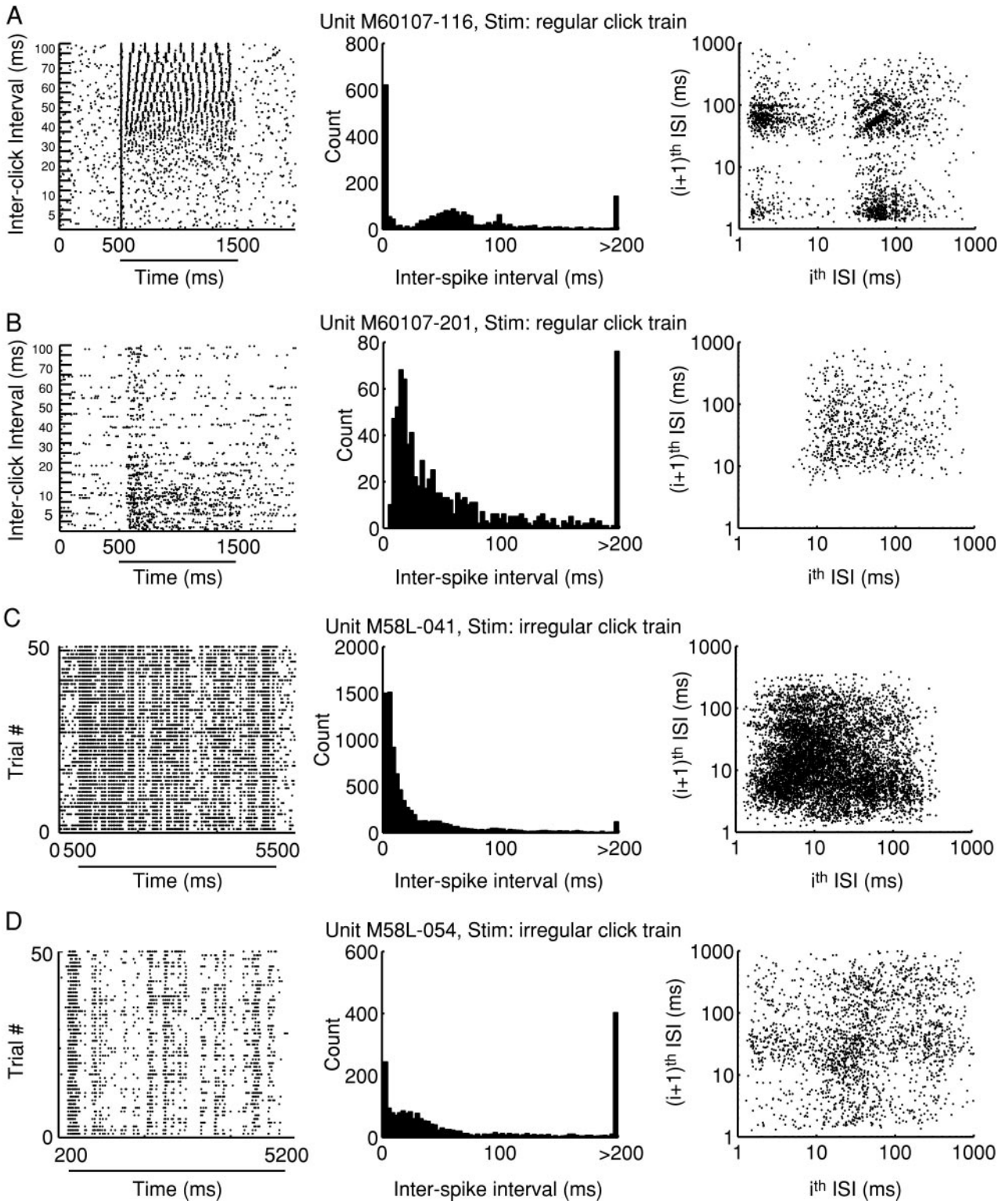

FIG. 1. Examples of temporal and rate coding in different stimulus domains (*A* and *B*) or the same domain by different populations (*C* and *D*). *Left*: dot raster plots. Time is on the abscissa, and the stimuli are ordered along the ordinate. Each point represents a single action potential. *Middle*: interspike interval (ISI) histogram. The histogram includes ISIs from all stimulus inter-click intervals (ICI) conditions. All data points in the tail of the histogram are lumped in the last bin. *Right*: ISIs are plotted against preceding ISI values. Stimulus conditions are indicated in each plot. *A*: example of a neuron with significant stimulus-synchronized discharges to regular click train stimuli. (*right*) Clusters of dots along the diagonal indicate responses that were synchronized to the regular click trains. *B*: example of a nonsynchronized, rate-response neuron with no significant stimulus-synchronized discharges to the regular click trains. In *A* and *B*, ICIs (ordinate) included 3, 5, 7.5, 10, 12.5, 15, 20, 25, 30, 35, 40, 45, 50, 55, 60, 65, 70, 75, and 100 ms. *C*: synchronized responses to 50 repetitions of an irregular click train (see METHODS). *D*: nonsynchronized responses to an irregular click train. The unit shown does not respond to the fine temporal structure as in *C*.

near 2–3 ms values (Fig. 1*A, right*). These clusters indicated short bursts of action potentials in response to each click stimulus. Bursting was present in almost all synchronized units we encountered. Both the diagonal bands and the bursting-associated clusters demonstrate the variety of temporal patterning of the neural spike trains in the synchronized response.

In contrast to the synchronized responses, a population of neurons was found to respond in a non-stimulus-synchronized manner such as the example in Fig. 1*B*. Units with responses of this type will be referred to as *nonsynchronized units*. The timing of the spikes appeared to be nearly random and unrelated to the timing of individual clicks in the click-train stimulus, and the ISI distribution appeared to be Poisson-like with a dead time (<5 ms) due to the unit's refractory period (Fig. 1*B, middle*). The conditional ISI plot for a nonsynchronized unit showed no clear clustering (Fig. 1*B, right*). Most of the ISIs were loosely distributed between 10 and 1,000 ms. In this case, ISIs of any length could be followed by ISIs of any other length, demonstrating the lack of structured temporal relationships between subsequent spikes to the preceding ones. Although not shown in this example, bursting can occur in nonsynchronized neurons as well.

The two types of temporal discharge patterns can also be demonstrated using irregular click trains (Fig. 1, *C* and *D*). For the synchronized unit example (Fig. 1*C*), discharges to multiple repetitions of the stimulus clearly show a repeatable temporal discharge synchronized to the timing structure of the click train (Fig. 1*C, left*), and clusters of points are visible in the conditional ISI plot (Fig. 1*C, right*). The nonsynchronized unit by comparison did not show any stimulus-synchronized structures in its responses to the same stimulus (Fig. 1*D, left*), and no strong ISI dependencies in the form of clustered points were observed (Fig. 1*D, right*).

Different neural populations, regardless of whether they were synchronized or nonsynchronized, encoded different temporal aspects of the stimuli within a short time window (Fig. 2, *A* vs. *B*). An example of a synchronized unit responding to ramped and damped sinusoidal stimuli is shown in Fig. 2*A*. The clustering in response to 25-ms stimulus intervals is clearly seen in both the ISI histogram (Fig. 2*A, middle*) and the conditional ISI plot (Fig. 2*A, right*). This unit responded preferentially to damped rather than ramped sinusoids at several half-lives (Fig. 2*A, left*). Preference to the ramped sinusoids was also observed in synchronized units (Lu et al. 2001a). The nonsynchronized unit in Fig. 2*B* responded to the same set of ramped and damped sinusoids with discharge patterns different from those in Fig. 2*A* as revealed by the ISI histogram (Fig. 2*B, middle*) and the conditional ISI plot (Fig. 2*B, right*). Clusters associated with temporal patterns at the 25-ms stimulus repetition period were absent (Fig. 2*B, right*). This unit responded preferentially to ramped than damped sinusoids (Fig. 2*B, left*). Preference to the damped sinusoids was also observed in nonsynchronized units (Lu et al. 2001a).

Figure 2, *C* and *D*, is a further example of the two response properties illustrated in Figs. 1 (*A–D*) and 2 (*A* and *B*), respectively, using sAM stimuli. Responses to each cycle of the sAM stimuli were generally more dispersed than responses to click stimuli (e.g., Fig. 1*A*). The stimulus-synchronized temporal patterns are nevertheless reflected as clusters in the conditional ISI plot (Fig. 2*C, right*). As with the other examples, the nonsynchronized responses to the sAM stimuli (Fig. 2*D, left*) did not show stimulus-related temporal patterns in either the ISI histogram (Fig. 2*D, middle*) or the conditional ISI plot (Fig. 2*D, right*). Both of these units, however, showed similar modulation frequency selectivity near 32 Hz based on their mean firing rates.

None of the examples of nonsynchronized units (Figs. 1, *B* and *D*, and 2, *B* and *D*) appeared to contain obvious temporal structures observable by dot-raster plots, ISI histograms, or conditional ISI plot. However, these analyses can overlook temporal structures quantifiable by more rigorous methods.

Information content based on the period histogram

The importance of spike timing for the representation of the click-train periodicity was analyzed in both synchronized and nonsynchronized units. Spike times were either systematically jittered or completely randomized, and their effects on the entropy, as defined by information theory (Shannon 1948), of the period histogram of the response was measured. This method quantifies the importance of coding by spike timing within a single stimulus period, e.g., ICI. Entropies that increased due to the manipulation would indicate that a nonrandom temporal pattern was present in a unit's response because a random spike train achieves maximum entropy.

We jittered the spike times of the responses systematically, from 3 to 100 ms, in the same step sizes as with the ICI, where the values given indicate the total width of the jitter. Figure 3*A* demonstrates the effect on the responses of a synchronized unit. The discharge rate was only slightly affected as some spikes were jittered out of the calculation window (Fig. 3*B, left*). More importantly, the Rayleigh statistic, a measure of how well the response was stimulus-synchronized, decreased with increasing jitter (Fig. 3*B, right*).

Because responses of synchronized units had stimulus-related temporal structures, increasing the amount of the jitter will systematically increase the entropy of the response (Fig. 3*C*). To facilitate comparisons, the entropies at each jitter value were normalized to the entropy at 100-ms jitter, where entropies were expected to be maximized using this analysis. For the synchronized units (black curves, each one representing responses at a particular ICI), the normalized entropy of the responses with no jitter (the lowest black curve) was ~0.8 to the click train of 100-ms ICI. As the jitter was increased, the entropy of the jittered responses increased monotonically from ~0.8 (no jitter) to ~1.0 (maximum jitter of 100 ms). Similar trends were observed for responses at other ICIs. In general, the entropy of responses increased with increasing ICI at a given jitter value and for responses with no jitter. These results highlight the fact that the spike times of the responses of synchronized units are crucial in representing timing information in the stimulus such as ICIs.

The same analysis was applied to the nonsynchronized population (Fig. 3*C*, gray curves). Unlike the synchronized population, the calculated entropy of the responses to any click train ICI was insensitive to spike-time jittering. It remained consistently near the value of 1. In contrast to the synchronized-population, there were little differences in the entropy values across the ICIs for both "no jitter" and jittered conditions. These results indicate that within stimulus periods, the spike timing of nonsynchronized neurons does not convey the information of click train ICI.

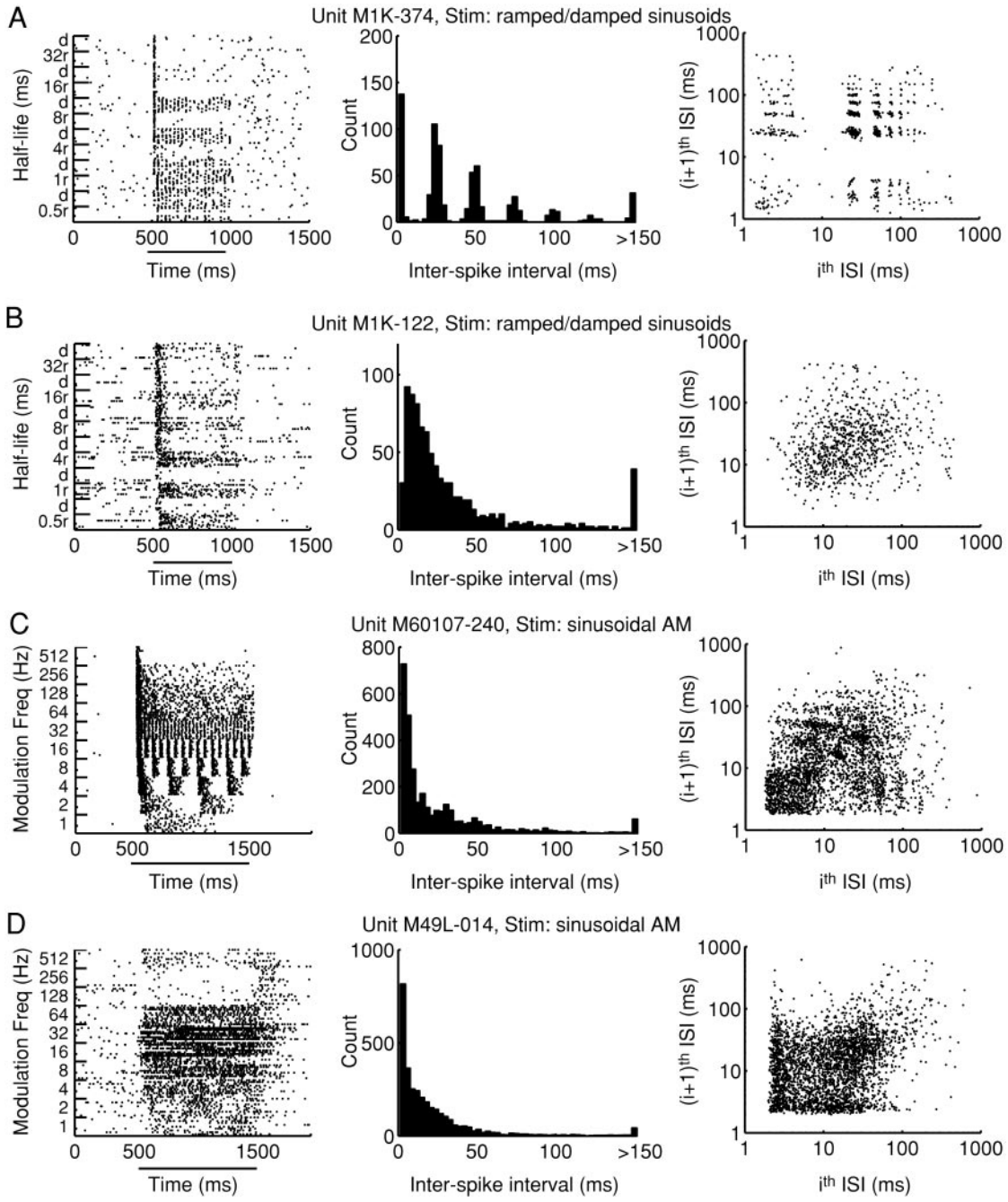

FIG. 2. Examples of temporal and rate coding of different stimulus aspects (*A* and *B*) and a further example of temporal and rate coding of the same stimulus domain by different populations (*C* and *D*). Format is the same as in Fig. 1. *A*: synchronized responses to ramped and damped sinusoids (see METHODS). *B*: nonsynchronized responses to ramped and damped sinusoids. In *A* and *B*, the letters r and d next to the half-life value (ordinate) indicate ramped or damped sinusoid, respectively. *C*: synchronized responses to sinusoidal amplitude modulated (sAM) stimuli. *D*: nonsynchronized responses to sAM stimuli.

Information content based on ISIs

To further explore the role of spike timing in two populations of cortical neurons, spike times over the duration of the stimulus were uniformly randomized, and the entropies of their ISI distributions were computed. The entropies of the unaltered spike times were then compared with those from the randomized version. The randomness, and therefore the entropy, of a spike train would increase if temporal structures were originally present in the spike train. The example in Fig. 4*A* shows the effect of this manipulation on a synchronized unit. The discharge rate remained the same (Fig. 4*A*, *middle*) but any synchronized responses were eliminated (Fig. 4*A*, *right*). The result of the randomization of spike times on the population of synchronized neurons was that they no longer had stimulus-synchronized spike trains (Fig. 4*B*). Average discharge rates, on the other hand, remained unchanged as compared with those based on unaltered spike trains (Fig. 4*B*, *inset*).

The ratio of the entropy of the unaltered spike train over the entropy of the randomized spike train was used as a measure to indicate the amount of spike timing information contained in a stimulus-evoked spike train. The average entropy ratio, calcu-

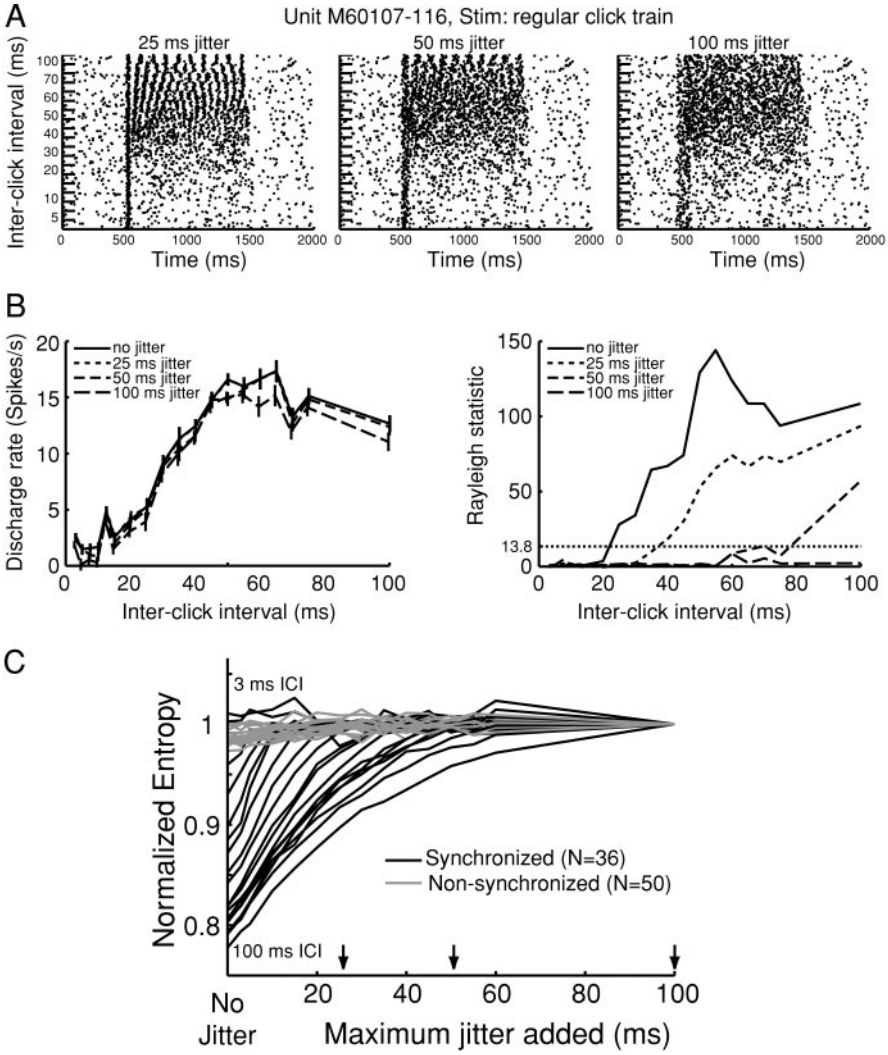

FIG. 3. Analysis of temporal coding capacity in the period histogram by spike time jittering. *A*: example dot raster plots of spike time jittering. Maximum jitters introduced were 25 ms (*left*), 50 ms (*middle*), and 100 ms (*right*). Unit showed stimulus-synchronization to regular click trains (Fig. 1*A*). *B*: effect of jittering on discharge rate (*left*) and Rayleigh statistic measures of stimulus synchronization (*right*). Values above 13.8 indicate statistically significant stimulus-synchronization. *C*: effects of spike time jittering on temporal coding. Maximum jitter introduced to the spike time is indicated on the *x* axis. Data from stimulus-synchronized neurons are shown in black curves. Nonsynchronized neurons are indicated in gray. Each curve represents the normalized average entropy of the population at a single stimulus ICI condition (from 3 to 100 ms). ↓, the jitter amounts used for the examples in *A* (25, 50, and 100 ms).

lated from the two populations of neurons, respectively, is plotted against the click train ICI (Fig. 4*C*, - ○ -, - + -). For comparison, the entropy ratio was also calculated for spontaneous discharges (Fig. 4*C*, - - -). Note that the entropy ratios for spontaneous discharges had values <1, indicating that spontaneous firing was not distributed completely randomly. In the case of the synchronized population (Fig. 4*C*, - ○ -), as the ICI increased, the entropy ratio began to drop near 30 ms (the mean ability of neurons to synchronize reported in Lu et al. 2001 was ~21 ms ICI) and became significantly different from the entropy ratio of spontaneous discharges at 50 ms. It continued to be significantly different for all larger values of ICI, having a value nearly 0.85 at 100 ms ICI. This difference in entropy ratios demonstrated that the randomness of the spike trains for the synchronized population was less than that of their randomized versions at ICIs longer than ~30 ms.

The curve for the average entropy ratio of the nonsynchronized population was fairly flat over the range of ICIs tested (Fig. 4*C*, - + -). In addition, none of the ratios were significantly different from that of the spontaneous discharges. The fact that the entropy ratio of the nonsynchronized population was consistently higher than that of spontaneous discharges across ICIs indicated that stimulus driven discharges in these neurons were at least as random as those of spontaneous firing.

Spike timing precision in two populations of neurons

We quantified the precision of spike timing of the responses to click train stimuli for each of the two populations of neurons and plotted the histogram of the CV for each population (Fig. 5). Figure 5*A* contains CVs from synchronized units for both regular and irregular click trains including all ICI conditions (median = 0.40, [25%, 75%] = [0.26, 0.54]). The subset of CVs corresponding to long ICIs (black bars, ≥100 ms for regular click trains and >150 ms for irregular click trains) were clustered at small values of CV (median = 0.34, [25%, 75%] = [0.20, 0.45]) indicating a smaller dispersion in the spike time when units responded to clicks separated by long ICIs.

In general, spike timing dispersion was smaller at stimulus onset than at successive stimulus events for an ongoing stimulus. In Fig. 5*B*, the CVs calculated from the onset responses (median = 0.22, [25%, 75%] = [0.13, 0.35]) of regular click trains were compared with the CVs calculated from the total responses (median = 0.30, [25%, 75%] = [0.15, 0.48]). We observed that, in general, CVs of the onset response were significantly ($P \ll 0.001$, Wilcoxon rank sum) smaller (Fig. 5*B*). In Fig. 5*C*, we analyze the CVs averaged over the population of neurons as a function of ICI. For regular click trains, the mean CV was ~0.2–0.3 at ICIs greater than ~30–40 ms

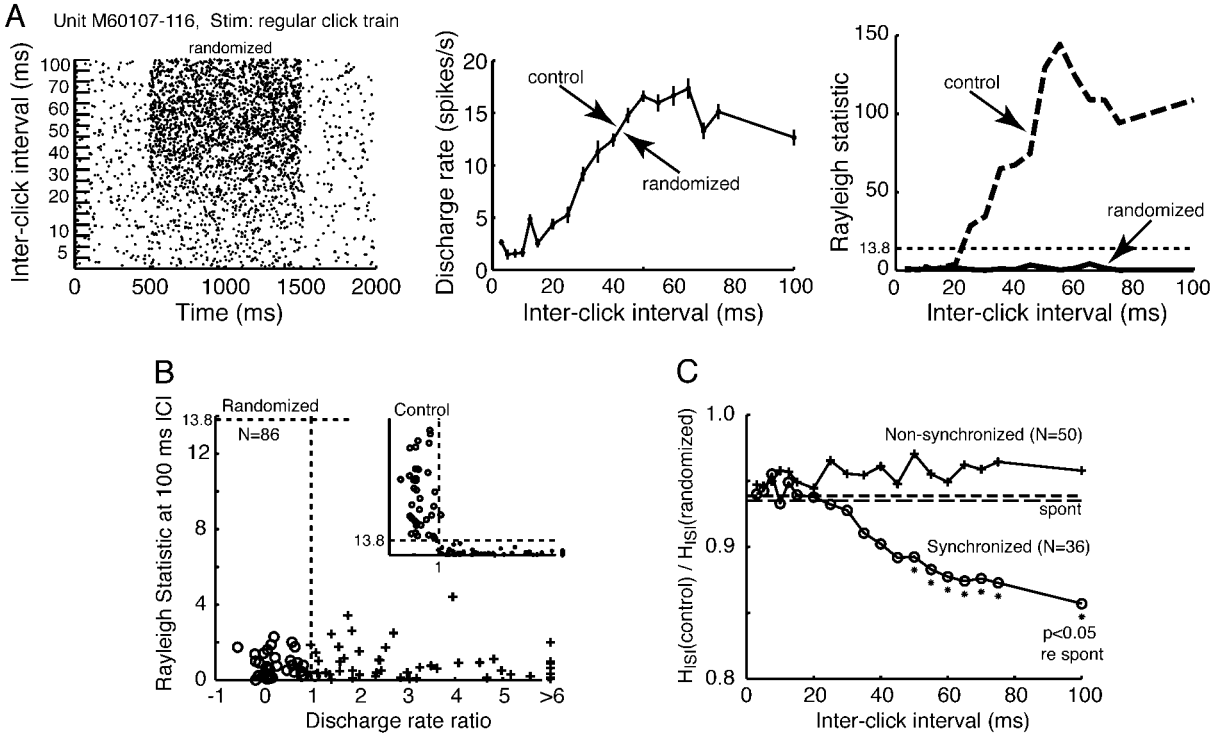

FIG. 4. Analysis by spike time randomization of temporal coding capacity of ISIs. *A*, *left*: dot raster of a unit after spike time randomization. This unit had stimulus-synchronization to regular click trains in its normal (control) responses (see Fig. 1*A*). *Middle*: effect of randomization on discharge rate. Curves from randomized and control responses overlap exactly. *Right*: effect of randomization on stimulus-synchronization measure, Rayleigh statistic. *B*: the effects of randomization on the 2 populations of neurons. ○, synchronized neurons; +, nonsynchronized neurons. The abscissa is the discharge rate ratio, the ratio of the discharge rate for a 3-ms ICI click train to that at 10 ms ICI. The ordinate is the Rayleigh statistic calculated at 100-ms ICI. Values above - - - indicate statistically significant stimulus-synchronization. *Inset*: the results from the unmodified control responses. *C*: entropy ratio of control to randomized spike times as a function of ICI for synchronized units (- ○ -) and nonsynchronized units (- + -), respectively. The curves represent the averaged entropy of the control divided by the average entropy of the randomized spike times. - - -, the entropy ratio computed from the spontaneous activity prior to the stimuli for synchronized and nonsynchronized units, respectively. Points that were significantly different from the entropy ratio of spontaneous activity are indicated with * ($P <$ 0.05, Wilcoxon rank sum).

and increased rapidly with decreasing ICIs (<30 ms). By 3 ms, the mean CV was near 0.6. It is noted that there was an inflection point in the curve near 25 ms in the mean CV of the population (Fig. 5*C*), which was also near the median synchronization boundary (21.3 ms) of the stimulus-synchronized population (Lu et al. 2001b). A similar trend was seen with the responses to irregular clicks, where the mean CV was ~0.35 at long ICIs and reached near 0.7 at short ICIs. The results shown in Fig. 5, *B* and *C*, indicate that, for synchronized units, spike time precision was higher in the onset response and in responses to more sparsely occurring stimulus events. Similar results were observed using both regular and irregular click trains.

The same analyses were applied to nonsynchronized units (Fig. 5, *right*). In contrast to synchronized units (Fig. 5*A*), there were proportionally fewer values of CVs <0.5 (median = 0.52, [25%, 75%] = [0.41, 0.58]; Fig. 5*D*), and the subset of CVs resulting from the longer ICIs (black bars) appears to be as widely distributed as the rest. Because many nonsynchronized neurons did not have a precise onset response, the data points for onset CV (median = 0.26, [25%, 75%] = [0.07, 0.50]) were widely scattered while the data points for the total CV (median = 0.53, [25%, 75%] = [0.44, 0.58]) tended to gather near 0.5 (Fig. 5*E*). There was a small drop in mean CV for the responses to the regular click trains with increasing ICIs (Fig. 5*F*, black curve), a reflection of these units' nonsynchronized responses. The responses to the irregular click trains showed a wide scatter but no systematic trend (Fig. 5*F*, gray curve). These results show that, compared with synchronized units, nonsynchronized units had greater spike timing dispersion in both onset (1st 50 ms window) and sustained responses.

Variation in spike count in two populations of neurons

The trial-to-trial variation in spike count was analyzed for both synchronized and nonsynchronized neurons. As with the latency, the histogram for the spike-count-based CVs is shown in Fig. 6*A* (median = 0.57, [25%, 75%] = [0.39, 0.86]). The subset of CVs calculated from the longer intervals (black bars) was not significantly lower. We also compared the CVs of the onset responses (median = 0.66, [25%, 75%] = [0.47, 0.94]) versus the CVs calculated from the total responses (median = 0.47, [25%, 75%] = [0.35, 0.70]; Fig. 6*B*). The median for onset CVs was significantly higher than that of the total CVs ($P \ll 0.001$, Wilcoxon rank sum), in contrast to the latency analysis (Fig. 5*B*), in which the opposite was observed. The values of the CVs for spike count were also considerably greater than those for spike latency. Whereas CVs for spike latency were always <1, there was a significant fraction of points for spike count CVs that were >1, indicating there was

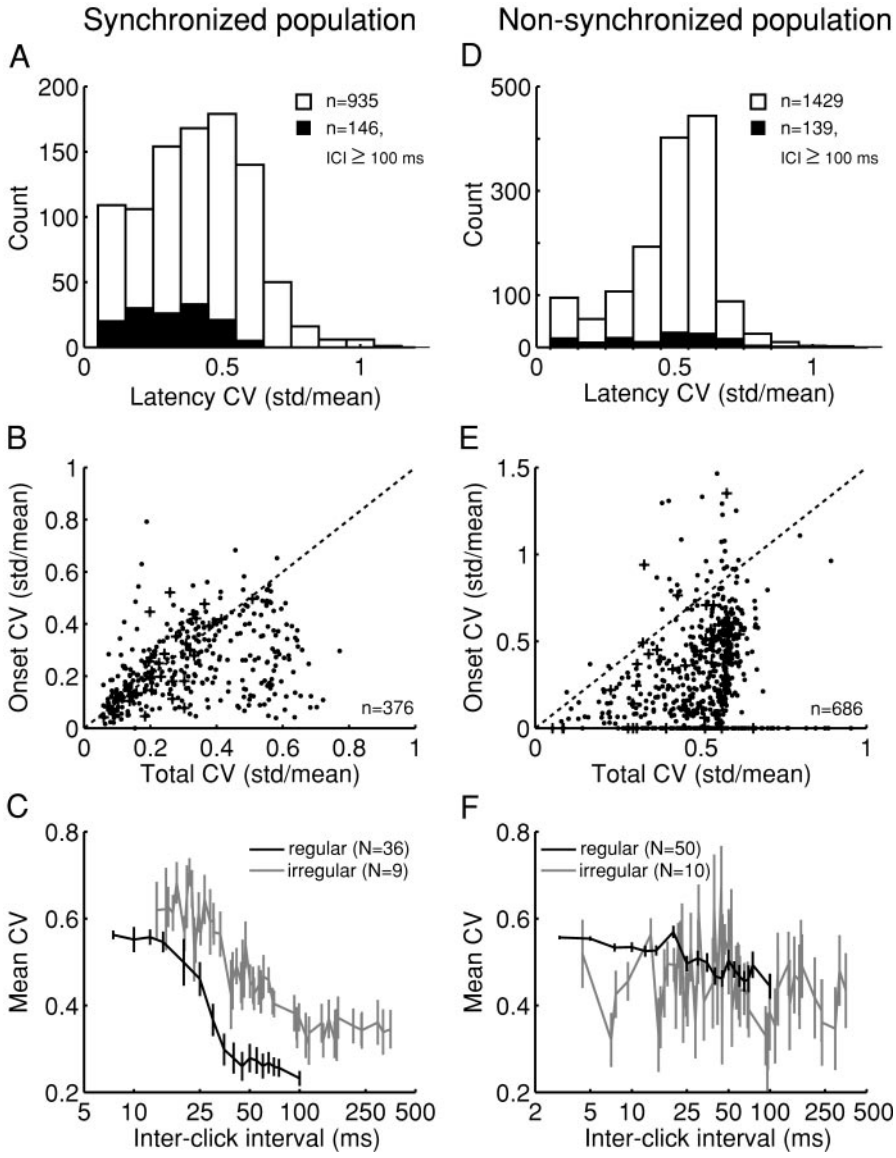

FIG. 5. Spike timing precision of responses to click-trains. *Left*: data from synchronized units; *right*: data from nonsynchronized units. *A*: distribution of CV (SD of the latency divided by mean latency) for regular click train responses. Spike latencies are relative to the click that evoked the response. Each CV is from a single stimulus ICI condition averaged over all clicks for each ICI. White bars, data pooled from both regular and irregular click trains (median = 0.40, [25%, 75%] = [0.26, 0.54]). Black bars, subset of responses to the ICIs ≥100 ms (median = 0.34, [25%, 75%] = [0.20, 0.45]). *B*: mean CV of the onset response vs. the mean CV of the total response to regular click trains. Each data point represents the response from a single stimulus ICI. Cross, responses to the 100-ms ICI click train. *C*: mean CV calculated from the responses to the regular (black) and irregular (gray) click trains as a function of ICI. Vertical bars indicate standard error of the mean (SE). *D–F*: same analyses as in *A–C* for the nonsynchronized units. *D*: pooled data from both regular and irregular click trains (white bars; median = 0.52, [25%, 75%] = [0.41, 0.57]). Subset of the responses to ICIs >100 ms (black bars; median = 0.51, [25%, 75%] = [0.30, 0.63]).

much more relative dispersion for the spike counts. The CV averaged over the population did not show the dependency on the inter-click interval for both regular click and irregular click trains (Fig. 6*C*).

The analyses were repeated for nonsynchronized neurons (Fig. 6, *right*). The histogram of the CVs were plotted as before (median = 1.4, [25%, 75%] = [0.90, 2.1]; Fig. 6*D*). A comparison of the onset CV (median = 1.37, [25%, 75%] = [0.81, 2.24]) with the total CV (median = 1.32, [25%, 75%] = [0.86, 1.82]) is shown in Fig. 6*E*. As mentioned before, many of the nonsynchronized neurons had unclear onset responses, which may also be responsible for the banding of points for the onset CV near 2, 3, and others. When the spike count CV was plotted as a function of ICI, we observed that the mean CV was smaller at shorter ICIs, where nonsynchronized neurons typically showed strong responses to the click-train stimuli (Fig. 6*F*, black curve). At the shortest ICI, the mean CV (Fig. 6*F*, black curve) was nearly the same as the mean CV found for the responses of the synchronized neurons (Fig. 6*C*). The trend was less clear for responses to irregular click trains (Fig. 6*F*, gray curve).

Information measures based on spike count and ISI

To quantify the capacity of these neurons to transmit information, the entropy and mutual information were calculated based on either trial-by-trial spike count or by ISIs. Figure 7 shows the distribution of entropy and mutual information based on both ISI and spike count measures, pooled from both populations. The ISI-based entropy, H_{ISI}, had a median of 6.52 [25%, 75%] = [5.87, 6.90] bits (Fig. 7*A*), whereas that for the spike-count-based measurement H_{SpkC} was 1.80 [25%, 75%] = [1.22, 2.57] bits (Fig. 7*B*). The distributions of mutual information had medians of 0.21 [25%, 75%] = [0.08, 0.50] bits for ISI-based calculations, I_{ISI} (Fig. 7*C*), and 0.07 [25%, 75%] = [0.04, 0.12] bits for spike-count-based measures, I_{SpkC} (Fig. 7*D*). These results indicate that ISI-based codes may potentially encode more information than spike-count-based codes.

Spike-count-based entropy was compared with the ISI-based entropy measured from the same unit for both synchronized and nonsynchronized population (Fig. 8). In Fig. 8*A*, the mean H_{ISI} and mean H_{SpkC} show a nonmonotonic relationship. At first, the entropies increase together until the mean H_{ISI} reaches

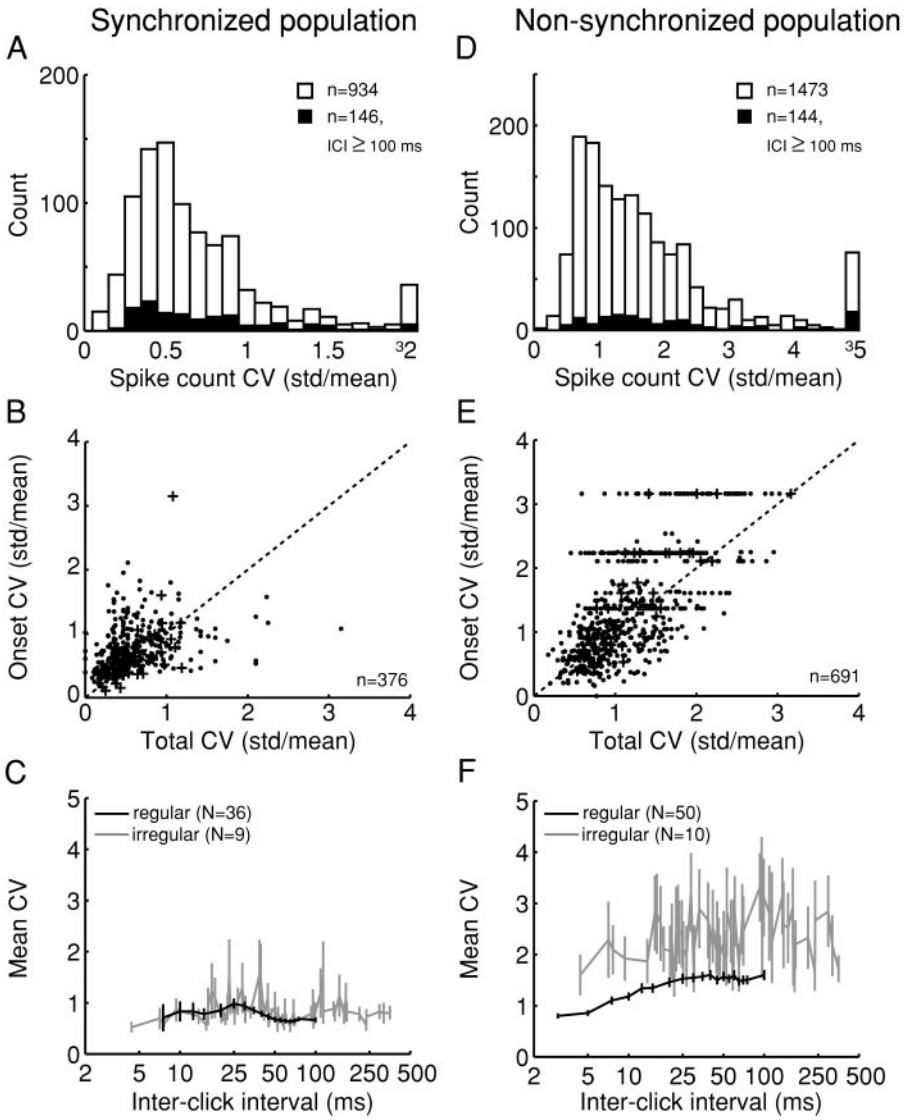

FIG. 6. Variation in spike count of responses to click trains. Format is the same as in Fig. 5. *A*: pooled data from both regular and irregular click trains (white bars; median = 0.57, [25%, 75%] = [0.39, 0.86]). Subset of responses to ICIs >100 ms (black bars; median = 0.68, [25%, 75%] = [0.43, 1.10]). *D*: pooled data from both regular and irregular click trains (white bars; median = 1.40, [25%, 75%] = [0.90, 2.10]). Subset of responses to ICIs ≥100 ms (black bars; median = 1.71, [25%, 75%] = [1.20, 2.65]).

a plateau near 5 bits. It is interesting to note that mean H_{SpkC} varied between 1 and 3 bits while there was little change in mean H_{ISI}. When the mutual information measures based on spike count and ISI were plotted against each other (Fig. 8*B*), there appeared to be little correlation, suggesting that information based on spike count or ISI was largely independent in the same neuron. There did not seem to be clusters based on whether or not units were from the synchronized or nonsynchronized populations in both analyses.

DISCUSSION

Temporal information in cortical responses

The current study investigates several issues not addressed in our previous reports (Liang et al. 2002; Lu et al. 2001a,b). The main issue concerns the possibility of temporal structures existing in the responses of the nonsynchronized neurons to time-varying stimuli such as click trains. Although our previous studies have shown that spike rate, but not stimulus synchrony-based measures, contained stimulus-specific information, we did not fully address whether additional information existed in these nonsynchronized neurons in the form of temporal coding not synchronized to stimulus period.

Based on the quantitative analyses reported here, there was not much indication of temporal coding beyond what is achieved with stimulus-synchronized responses in auditory cortical responses to repetitive stimulus events. We found little evidence of cortical coding based on ISIs that was not directly stimulus-synchronized. Unlike the responses for the synchronized neurons, we observed that nonsynchronized rate-response neurons did not show a significant increase in entropy when the spike times were jittered or randomized. In fact, the spike timing in these neurons appeared to be nearly as random as that of spontaneous discharges (Fig. 4*C*). Although temporal discharge patterns based on ISI could potentially code more information than spike-count-based measures in nonsynchronized neurons, it remains unclear whether and how such information is used by the auditory cortex. The possibility cannot be ruled out that temporal coding, not detectable by our present analyses and data set, may be used by auditory cortical neurons to encode finer temporal or spectral changes in a complex sound or sound sequences than those tested in our studies.

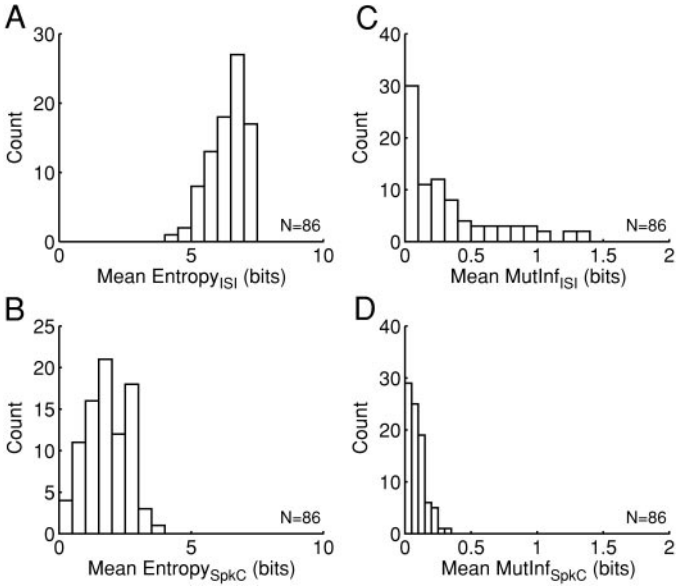

FIG. 7. Histograms of entropy and mutual information of responses to click trains. *A*: entropy of ISI distribution. Median = 6.52, [25%, 75%] = [5.87, 6.90] bits. *B*: spike-count-based entropy. Median = 1.80, [25%, 75%] = [1.22, 2.57] bits. *C*: mutual information of ISI. Median = 0.21, [25%, 75%] = [0.08, 0.50] bits. *D*: spike-count-based mutual information. Median = 0.07, [25%, 75%] = [0.04, 0.12] bits.

In summary, the experimental observations from our previous studies and theoretical analyses of the present study lead to the following conclusions. First, temporal and rate coding may operate at separate stimulus domains, encode the same stimulus space in parallel by different neuronal populations, or encode different stimulus aspects. Second, spike timing, but not mean firing rate, is crucial to encode stimulus periodicity in "synchronized" neurons. Third, "nonsynchronized" neurons contain no clear spike timing information for encoding stimulus periodicity. These neurons exhibit a transformed representation of the stimulus in the auditory cortex and deserve greater attention in future studies. Fourth, spike timing on the occurrence of stimulus events is more precise at the first event (onset) than at successive ones, and at sparsely occurring stimulus events than at densely occurring stimulus events.

Statistical variations of spike timing and count in onset and sustained responses

Because the reproducibility of responses is an important factor in considering potential neural codes, we studied the relative dispersion of both spike time precision and spike count variation in responses to click trains (Figs. 5 and 6). The results of the CV analysis have implications for both the spike time latency reported in the literature and the inferences that can be drawn from them to extrapolate to whole stimulus encoding. Although it has been shown that the precision of the first spike latency can be well preserved from the auditory nerve to A1 (Heil and Irvine 1997), the timing precision of subsequent responses to an ongoing stimulus has not been addressed. This may be due, in large part, to the phasic responses that dominate anesthetized auditory cortex, the preparation with which many previous studies of onset responses were conducted (e.g., Heil 1997a,b; Phillips and Hall 1990). Because of this, and the more limited synchronizing capability of neurons in anesthetized than awake auditory cortex (Goldstein et al. 1959), the issue of temporal precision of auditory cortical neurons during an ongoing stimulus was difficult to address.

For the synchronized neurons, we found that spike time dispersion was generally smaller in onset responses and in the responses to sparsely occurring acoustic events (separated by $>30-40$ ms) than in the responses to densely occurring acoustic events (Fig. 5, *B* and *C*). These findings held for click trains with either static (regular) or dynamic (irregular) ICIs. The latter was used to reduce potential effects of adaptation. As shown in Fig. 5, spike time precision is much reduced in the responses of nonsynchronized neurons. This is consistent with the suggestion that these neurons use their firing rates instead to encode stimulus parameters (Lu et al. 2001b).

The CV analysis of spike count showed a much larger relative scatter than with the spike latency (Fig. 6). We found that there was no clear correlation between spike count CV and click-train ICI (Fig. 6*C*) for synchronized neurons. In the case of nonsynchronized neurons, there was indeed a correlation (Fig. 6*F*), where CV values were smaller with shorter ICIs. These results mirror those for the spike timing (Fig. 5, *C* and *F*), where the respective operating domains (long vs. short ICIs) for each type of neuron (synchronized vs. nonsynchronized) have smaller CV values but only for the proper coding method (spike time vs. spike count).

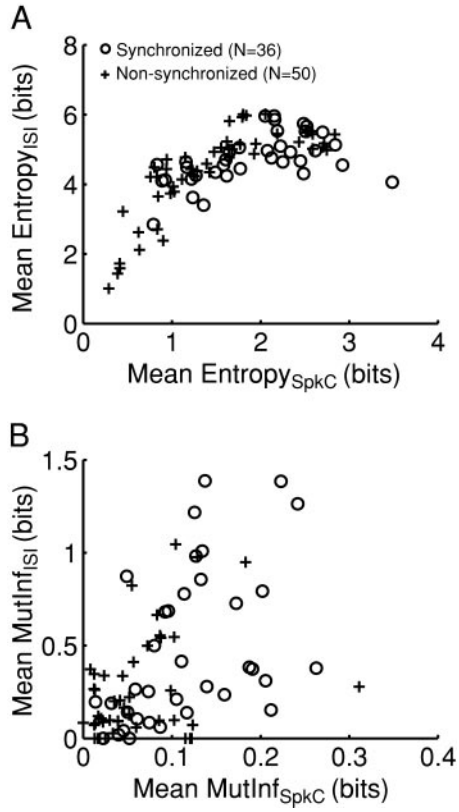

FIG. 8. Comparison between information measures based on ISI and spike count. Each data point represents a single click-train ICI condition. ○, data from synchronized units; +, data from nonsynchronized units. *A*: ISI based entropy is plotted against spike-count-based entropy. *B*: ISI-based mutual information is plotted against spike-count-based mutual information.

Effects of neuronal adaptation on information measures

Neuronal adaptation (a change in response strength as a function of time) may potentially affect the calculation of the entropy and mutual information that was based on the entire stimulus duration. Adaptation typically occurs prominently within the first 100 ms of the response, usually as part of an onset burst. In Fig. 9, we compared the entropy and mutual information for both spike count and ISI measures between the first and second half of the response, both with (Fig. 9, *A* and *B*) and without (Fig. 9, *C* and *D*) the discharges within the first 100 ms (onset spikes). The entropies were closely correlated between the two halves of the response (Fig. 9, *A* and *C*). The slopes of the linear fits of the data points in Fig. 9, *A* and *C*, were 0.84 (*all spikes*) and 0.95 (*without onset spikes*) for ISI measures and 0.96 (*all spikes*) and 1.01 (*without onset spikes*) for spike count measures. Although the slight shift in Fig. 9*A* for the spike-count-based entropy (as compared with Fig. 9*C*) suggests that the onset response can cause the entropy to be overestimated in some cases, there is little evidence of adaptation such that the entropy measures of the second half of the response are much smaller than those of the first half. Figure 9*C* shows that sustained responses (after onset spikes) had consistent values of entropy throughout stimulus duration, suggesting that adaptation is not a significant factor for the majority of sustained responses that we recorded in awake marmoset auditory cortex. Many examples of highly sustained discharges for various time-varying stimuli have been shown in our prior studies (e.g., Liang et al. 2002; Lu et al. 2001a,b). The comparison of the mutual information measures between the first and second half of responses (Fig. 9, *B* and *D*) also showed similar trends as the entropies. The slopes of the linear fits of the data points in Fig. 9, *B* and *D*, were 0.68 (*all spikes*) and 0.74 (*without onset spikes*) for ISI measures and 0.96 (*all spikes*) and 0.96 (*without onset spikes*) for spike count measures, respectively.

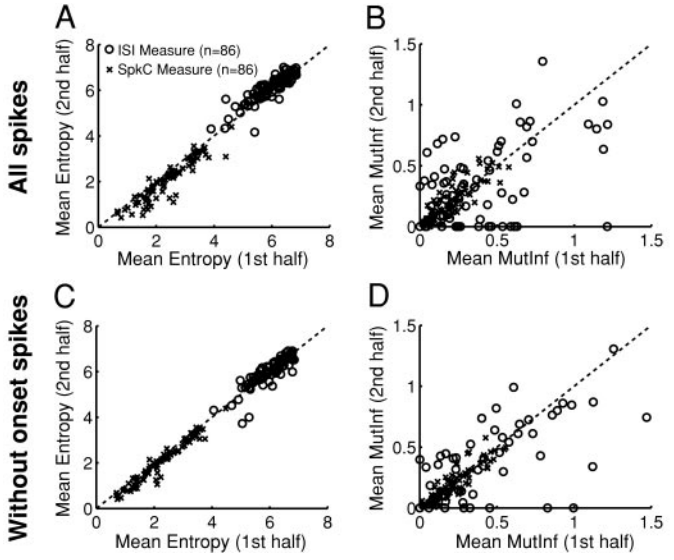

FIG. 9. Effects of neuronal adaptation on information measures. Data shown are pooled from synchronized and nonsynchronized units. ○, ISI measures. ×, spike count measures. - - -, a slope of 1.0. *A* and *B*: mean entropy and mutual information of the 1st half (0–500 ms) vs. the 2nd half (500–1,000 ms) of responses to click trains, respectively. The slopes of the linear fits were: 0.84 (ISI-entropy), 0.96 (spike count-entropy), 0.68 (ISI-mutual information), and 0.96 (spike count-mutual information). *C* and *D*: mean entropy and mutual information of the 1st half (100–550 ms) vs. the 2nd half (550–1,000 ms) of the sustained response (without onset spikes), respectively. The slopes of the linear fits were: 0.95 (ISI-entropy), 1.01 (spike count-entropy), 0.74 (ISI-mutual information), and 0.96 (spike count-mutual information).

Comparison with other studies

The values that we found for both the ISI and spike-count entropies (0–8 bits) and mutual information (0–1.6 bits) were comparable to published data from other studies of cortical neurons. The range of information rates reported in the literature for the cortex is large due in part to the different stimulus ensembles used. Neurons in the inferior temporal area in alert macaques were reported to have an information rate of 1 bits/s (Optican and Richmond 1987). It was shown that V1 neurons can transmit 5–30 bits/s with 25% efficiency in response to pseudorandom stimuli and that spikes with short ISIs carried a disproportionate amount of information (Reich et al. 2000). The rate of information transmission was reported in MT of alert macaque monkeys to be ~1 bit/s for constant stimuli to 12 bits/s and as high as 29 bits/s for variable stimuli (Buracas et al. 1998). In the orbitofrontal cortex of primates, it was 0.09 bits for olfactory neurons (Rolls et al. 1996). Primate temporal cortex was shown to have a range of ~0.4–1.2 bits (Tovee et al. 1993). It is possible that variations in the information theoretic analyses are attributed to the cortical area recorded from as well as the stimuli used.

Some previous methods computed the first few principal components and used those values as a basis for the information measure (Optican and Richmond 1987; Rolls et al. 1996; Tovee et al. 1993). Currently, one of the more predominant methods involves representing the number and spacing of spikes with binary strings (de Ruyter van Steveninck et al. 1997; Reinagel and Reid 2000; Rieke et al. 1998). The information content is then calculated from the frequency distribution of the resulting strings. Although calculating the information content based on binary strings could, in theory, account for all possible temporal patterns, it can be difficult to do in practice because of the enormous amount of data required to estimate the frequency of occurrence of particular words. The number of stimulus presentations used in our experimental protocols was too few to adequately and robustly calculate information based on binary strings (de Ruyter van Steveninck et al. 1997; Rieke et al. 1998; Warzecha and Egelhaaf 1999). The approach taken here was better suited to our existing data set.

We observed little evidence indicating any reliable temporal structure (based on ISIs) in the responses to rapidly modulated stimuli, but the information calculations of ISI in the present study did not take into account absolute spike time relative to stimulus onset (i.e., latency). As shown in a somatosensory cortex study, the location of whisker stimulation can be encoded by the latency of the response (Panzeri et al. 2001). The authors in that study concluded that the temporal information in their data appeared to be based mainly on the response latency. However, because the responses they observed consisted of largely onset discharges recorded in deeply anesthetized animals, their conclusion regarding the role of spike timing cannot be generalized to situations where there is an abundance of sustained discharges, such as the nonsynchro-

nized responses we have observed in the auditory cortex of awake primates.

The contribution of our present study is to demonstrate that coding by cortical neurons is not simply an issue of rate code versus temporal code, but *when* each of the coding methods is put into use and by *which* population of cortical neurons.

ACKNOWLEDGMENTS

We thank Drs. K. Johnson, O. Donchin, and K. Zhang and C. DiMattina, and S. Sadagopan for helpful comments on the manuscript and A. Pistorio for proofreading, graphic work, and assistance with animal training.

GRANTS

This work was supported by National Institute on Deafness and Other Communication Disorders Grant DC-03180, a Presidential Early Career Award for Scientists and Engineers (X. Wang), and a grant from the National Organization for Hearing Research Foundation.

REFERENCES

Adrian ED and Zotterman Y. The impulses produced by sensory nerve endings. II. The response of a single end organ. *J Physiol* 61: 151–171, 1926.

Aitkin LM, Merzenich MM, Irvine DR, Clarey JC, and Nelson JE. Frequency representation in auditory cortex of the common marmoset (*Callithrix jacchus jacchus*). *J Comp Neurol* 252: 175–185, 1986.

Barbour DB and Wang X. Temporal coherence sensitivity in auditory cortex. *J Neurophysiol* 88: 2684–2699, 2002.

Bieser A and Müller-Preuss P. Auditory responsive cortex in the squirrel monkey: neural responses to amplitude-modulated sounds. *Exp Brain Res* 108: 273–284, 1996.

Borst A and Theunissen FE. Information theory and neural coding. *Nat Neurosci* 2: 947–957, 1999.

Buracas GT, Zador AM, DeWeese MR, and Albright TD. Efficient discrimination of temporal patterns by motion-sensitive neurons in primate visual cortex. *Neuron* 20: 959–969, 1998.

Creutzfeldt O, Hellweg F-C, and Schreiner C. Thalamocortical transformation of responses to complex auditory stimuli. *Exp Brain Res* 39: 87–104, 1980.

deCharms RC, Blake DT, and Merzenich MM. Optimizing sound features for cortical neurons. *Science* 280: 1439–1443, 1998.

de Ribaupierre F, Goldstein MH Jr, and Yeni-Komshian G. Cortical coding of repetitive acoustic pulses. *Brain Res* 48: 205–225, 1972.

de Ruyter van Steveninck RR, Lewen GD, Strong SP, Koberle R, and Bialek W. Reproducibility and variability in neural spike trains. *Science* 275: 1805–1808, 1997.

Eggermont JJ. Rate and synchronization measures of periodicity coding in cat primary auditory cortex. *Hear Res* 56: 153–167, 1991.

Furukawa S and Middlebrooks JC. Cortical representation of auditory space: information-bearing features of spike patterns. *J Neurophysiol* 87: 1749–1762, 2002.

Goldstein MH Jr, Kiang NY-S, and Brown RM. Response of the auditory cortex to repetitive acoustic stimuli. *J Acoust Soc Am* 31: 356–364, 1959.

Heil P. Auditory cortical onset responses revisited. I. First-spike timing. *J Neurophysiol* 77: 2616–2641, 1997a.

Heil P. Auditory cortical onset responses revisited. II. Response strength. *J Neurophysiol* 77: 2642–2660, 1997b.

Heil P and Irvine DR. First-spike timing of auditory-nerve fibers and comparison with auditory cortex. *J Neurophysiol* 78: 2438–2454, 1997.

Johnson DH. The relationship between spike rate and synchrony in responses of auditory-nerve fibers to single tones. *J Acoust Soc Am* 68: 1115–1122, 1980.

Joris PX and Yin TCT. Responses to amplitude-modulated tones in the auditory nerve of the cat. *J Acoust Soc Am* 91: 215–232, 1992.

Langner G. Periodicity coding in the auditory system. *Hear Res* 60: 115–142, 1992.

Laurent G, Wehr M, and Davidowitz H. Temporal representations of odors in an olfactory network. *J Neurosci* 16: 3837–3847, 1996.

Liang L, Lu T, and Wang X. Neural representations of sinusoidal amplitude and frequency modulations in the primary auditory cortex of awake primates. *J Neurophysiol* 87: 2237–2261, 2002.

Lu T, Liang L, and Wang X. Neural representations of temporally asymmetric stimuli in the auditory cortex of awake primates. *J Neurophysiol* 85: 2364–2380, 2001a.

Lu T, Liang L, and Wang X. Temporal and rate representations of time-varying signals in the auditory cortex of awake primates. *Nat Neurosci* 4: 1131–1138, 2001b.

Lu T and Wang X. Temporal discharge patterns evoked by rapid sequences of wide- and narrowband clicks in the primary auditory cortex of cat. *J Neurophysiol* 84: 236–246, 2000.

Malone BJ, Scott BH, and Semple MN. Context-dependent adaptive coding of interaural phase disparity in the auditory cortex of awake macaques. *J Neurosci.* 22: 4625–4638, 2002.

Optican LM and Richmond BJ. Temporal encoding of two-dimensional patterns by single units in primate inferior temporal cortex. III. Information theoretic analysis. *J Neurophysiol* 57: 162–178, 1987.

Panzeri S, Petersen RS, Schultz SR, Lebedev M, and Diamond ME. The role of spike timing in the coding of stimulus location in rat somatosensory cortex. *Neuron* 29: 769–777, 2001.

Panzeri S and Treves A. Analytical estimates of limited sampling biases in different information measures. *Network Comput Neural Syst* 7: 87–107, 1996.

Patterson RD. The sound of a sinusoid: spectral models. *J Acoust Soc Am*, 96: 1409–1418, 1994.

Phillips DP and Hall SE. Response timing constraints on the cortical representation of sound time structure. *J Acoust Soc Am* 88: 1403–1411, 1990.

Phillips DP, Hall SE, and Hollett JL. Repetition rate and signal level effects on neuronal responses to brief tone pulses in cat auditory cortex. *J Acoust Soc Am* 85: 2537–2549, 1989.

Recanzone GH. Response profiles of auditory cortical neurons to tones and noise in behaving macaque monkeys. *Hear Res* 150: 104–118, 2000.

Reich DS, Mechler F, Purpura KP, and Victor JD. Interspike intervals, receptive fields, and information encoding in primary visual cortex. *J Neurosci* 20: 1964–1974, 2000.

Reinagel P and Reid RC. Temporal coding of visual information in the thalamus. *J Neurosci* 20: 5392–5400, 2000.

Rieke F, Warland D, de Ruyter van Steveninck R, and Bialek W. *Spikes: Exploring the Neural Code.* Cambridge, MA: MIT Press, 1998.

Rolls ET, Critchley HD, and Treves A. Representation of olfactory information in the primate orbitofrontal cortex. *J Neurophysiol*, 75: 1982–1996, 1996.

Shannon CE. A mathematical theory of communication. *Bell Syst Tech J* 27: 379–423, 623–656, 1948.

Tovee MJ, Rolls ET, Treves A, and Bellis RP. Information encoding and the responses of single neurons in the primate temporal visual cortex. *J Neurophysiol* 70: 640–654, 1993.

Wang X. On cortical coding of vocal communication sounds in primates. *Proc Natl Acad Sci USA* 97: 11843–11849, 2000.

Wang X, Lu T, and Liang L. Cortical processing of temporal modulations. *Speech Commun* 41: 107–121, 2003.

Warzecha AK and Egelhaaf M. Variability in spike trains during constant and dynamic stimulation. *Science* 283: 1927–1930, 1999.

Whitfield IC and Evans EF. Responses of auditory cortical neurons to stimuli of changing frequency. *J Neurophysiol* 28: 655–672, 1965.